

# Effect of GNFs/Al Interfacial Characteristics on the Mechanical Properties of Graphene Nanoflakes Reinforced Aluminum Matrix Composites

S Z Zhao, S J Yan \*, X Chen and S L Dai

Beijing Institute of Aeronautical Materials, Beijing100095, PR China

\* Corresponding author's e-mail address: shaojiuyan@126.com

**Abstract.** Graphene nanoflakes-reinforced aluminum matrix composites (GNFs/Al) with 1.0 wt.% GNFs were fabricated by a spark plasma sintering (SPS) method under two different condition. The microstructural and interfacial characteristics of the two composites were systematically investigated, and their different tensile mechanical properties were found to depend strongly on the GNFs/Al interfacial characteristics. Prolonged sintering in SPS should be avoided as it promotes obvious interfacial reaction that degrades the mechanical properties. The enhanced mechanical properties of the GNFs/Al composites in this study can be ascribed to their exquisite microstructures, specifically the well-maintained structure of raw reinforcement, the uniform GNF distribution and their parallel alignment with the tensile direction, the absence of mass interfacial reaction, and the good interface bonding.

## 1. Introduction

Graphene is a perfect two-dimensional (2-D) lattice of carbon atoms [1], which has become the focus of scientific research as its unique structure and superior properties [2-4]. Graphene nanoflakes (GNFs) which compose of a few graphene layers and possess similar properties of single-layer graphene, is much easier to produce and handle. Current researches have applied GNFs to strengthen various polymer, ceramic, and metal matrix composites [5-7]. On the other hand, aluminum and aluminum alloys are among the key materials in aerospace and military vehicles due to their low density; however, their uses are limited by their relatively low strength. Since the graphene-reinforced aluminum composites are expected to be both lighter and stronger, methods to fabricate such composites are greatly desired.

In recent years, some researchers have attempt to fabricated GNFs reinforced aluminum or its alloy composites [8-13]. Their results are quite different. Shin make the composites two times higher than that of monolithic Al with an addition of only 0.7 vol. % GNFs [11], while some results show that GNFs ruin the strength of the matrix [8]. Most of the present researches have been focused on preparation and mechanical properties of GNFs reinforced aluminum composites. However, investigation on interface is not thorough and some results even contradict because of the complexity associated with the interfacial reaction between graphene and Al matrix. As the interface characteristic have crucial effect on properties of composites, then elaborate study on the interface of the composites is essential. As the reactions between graphene and other elements in the alloys could create more complex composites, it is difficult to analyse the strengthening mechanism in composites with



aluminum alloy matrices. Therefore, in this study we selected pure aluminum instead of aluminum alloys as the matrix.

## 2. Materials and experimental procedures

### 2.1. Fabrication of GNFs/Al composites

Ball milling was employed to disperse 1.0 wt. % GNFs into aluminum powders to obtain GNFs/Al mixtures. First, 5 g of GNFs was dispersed in ethanol by ultrasonication. The solution and 500 g of aluminum powders were poured into a stainless-steel jar, and mixed by ball milling without any dispersive agents. Hardened stainless-steel balls 3 mm in diameter were used in the milling process (100 rpm and 20 h), with the mass ratio between the ball and material being 10:1. Last, the milled slurry was dried in a vacuum furnace at 60 °C for 10 h.

Fig. 1 gives the low- and high-magnification SEM images of the GNFs/Al mixture. Fig. 1 (a) shows that the aluminum powders are flakes with 20  $\mu\text{m}$  in diameter after milling. In Fig. 1(b), the high-magnification image shows that the aluminum powders were wrapped by GNFs, which indicates the even dispersion of GNFs into aluminum powders.

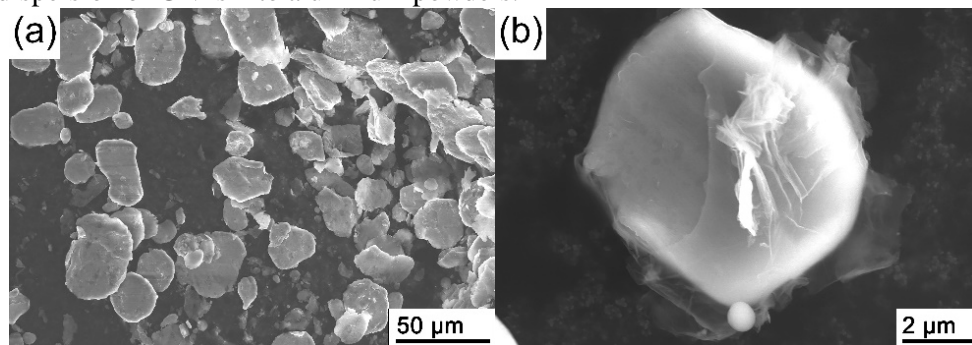


**Fig. 1** SEM images of the mixed GNFs/Al powders after milling  
(a) low-magnification and (b) high-magnification

SPS was used to fabricate the bulk GNFs/Al composites. The dried GNFs/Al mixture was placed in a graphite die with inner diameter of 30 mm, and then sintered at 560 °C for 4 or 8 min under a maintained pressure of 30 MPa. The sintering time was varied to obtain composites with distinct microstructures and therefore different mechanical properties. The formed bulk GNFs/Al composites were disc-shaped, 30 mm in diameter and 8 mm in thickness. For comparison, pure aluminum specimens were also prepared by the same process.

### 2.2. Tensile test and microscopy analysis

The density of the bulk materials was measured by Archimedes principle. The tensile mechanical properties of the bulk samples were determined by a testing machine (Instron 5887) at ambient temperature using a displacement rate of 1 mm/min. For minimizing the experimental error, three tensile specimens were cut from each sample along the radial direction with dog bone shape (thickness: 2 mm, gauge length: 10 mm, gauge width: 3 mm). A Hitachi S-4800 SEM system was employed to examine the fracture surface of the specimens after tensile tests. The substructure features and interface characteristics of the composites were observed using a Tecnai G2 F30 transmission electron microscopy (TEM) system. The presence of graphene in the composites was confirmed by Raman spectra (HORIBA LabRAM HR800) using an excitation wavelength of 514 nm.

### 3. Results and discussion

#### 3.1. Tensile properties

The relative densities of all tested samples, including pure Al and GNFs/Al composites, are all near 100% of the theoretical values. Therefore, the influence of the sintered density on the mechanical properties is neglected. For clarity, the samples are coded according to the sintering time, with the 4-min-sintered bulk materials named “I” and the 8-min-sintered ones named “II”.

The tensile test results shown in Table 1 indicate that the sintering time has a distinct influence on the mechanical properties of the GNFs/Al composites, although it has little effect on pure Al. Compared with the tensile strength (111 MPa) and yield strength (61 MPa) of the 4-min-sintered Pure Al I, those of the 4-min-sintered Composite I are enhanced by 42% and 41%, respectively. In terms of ductility, the elongation of Composite I retains the relative high value of around 14.5%, although it is only half that of Pure Al I. On the other hand, compared with the 8-min-sintered Pure Al II, the strength of the 8-min-sintered Composite II changes very little while its elongation declines to just 9.5%. The above results suggest that the fabrication process has an impact on the microstructure and therefore mechanical properties of the GNFs/Al composites.

**Table 1** The average tensile values of GNFs/Al composite and pure Al samples with different sintering times.

| Material     | Tensile Strength (MPa) | Yield Strength (MPa) | Elongation (%) | Sintering time (min) |
|--------------|------------------------|----------------------|----------------|----------------------|
| Composite I  | 158±4                  | 86±5                 | 14.5±0.5       | 4                    |
| Composite II | 107±4                  | 55±5                 | 9.5±0.8        | 8                    |
| Pure Al I    | 111±2                  | 61±3                 | 26.2±0.3       | 4                    |
| Pure Al II   | 105±3                  | 56.6±3               | 27.5±0.5       | 8                    |

#### 3.2. Fracture surface morphology

Fig. 2 shows the low- and high-magnification SEM images of the tensile fracture surface of Composite I, Composite II, and Pure Al I after tensile tests. As the mechanical properties of Pure Al I and II are almost the same, only Pure Al I was considered in the study of fracture surface morphology as well as the TEM study (to be discussed later). The low-magnification images in Fig. 2 exhibit obviously distinct morphologies among these three fracture surfaces. The fracture surface of Composite I presents an obvious lamellar structure, while those of Composite II and Pure Al I are full of dimple-like structures and dimples, respectively. Besides, some fragments are distributed on the fracture surface of Composite II, which can be speculated to be the  $\text{Al}_4\text{C}_3$  phase formed in interface reaction according to the TEM observation (to be discussed later). The interface reaction phase can strongly enhance the interface bonding and hence the fracture surface of Composite II is full of dimple-like structure. The high-magnification images in Fig. 2 exhibit lamella structure in both Composite I and II, while that of Pure Al I is full of dimples. In sum, the fracture surface of Composite II is composed of dimple-like structures with some lamellar structures on the dimple edge, showing a transition from the obvious lamellar structure in Composite I to the dimples in Pure Al I.

The high-magnification images in Fig. 2 also show that the GNFs are pulled out along with the aluminum lamellas on the fracture surfaces of Composite I and II. It is also worth noting that the pulled-out GNFs appear smooth, which is distinct from their original wrinkled feature (Fig. 1b). This clearly indicates that the GNFs still endured tensile stress even after the aluminum matrix fractured, leading to their unfolding. In addition, the length of the pulled-out GNFs in Composite II is much shorter than that in Composite I. Previous studies on carbon fiber-reinforced aluminum composites revealed that the fracture behavior of composites depends dramatically on the type of the reinforcement-matrix interface. When the interface between the carbon fiber and matrix is relatively weak, cracks grow at the interface; and when the cracks cross the fiber, long pulled-out carbon fibers

appear [14]. When the interface is relatively strong, the propagation of cracks along the interface is reduced, resulting in a shorter pulled-out length of the fibers [14]. When the interface is very strong with the formation of brittle compounds, the fracture surface is flat without the pulled-out fibers [15]. Although the length of the pulled-out GNFs in Composite I is approximately 20–50 nm, which is longer than that in Composite II (less than 20 nm), it is much less than that of the original GNFs (ca. 50  $\mu\text{m}$ ) used as raw material in this study. Therefore, the interface between the GNFs and matrix in Composite I is relatively strong. In Composite II, the much shorter pulled-out GNFs, coupled with the dimple-like structure in the fracture surface, indicate that the interface is even stronger than that in Composite I due to the interface reaction. However, although this reaction enhances the interface in Composite II, the elongation is much less than that of pure Al, because  $\text{Al}_4\text{C}_3$  is brittle.

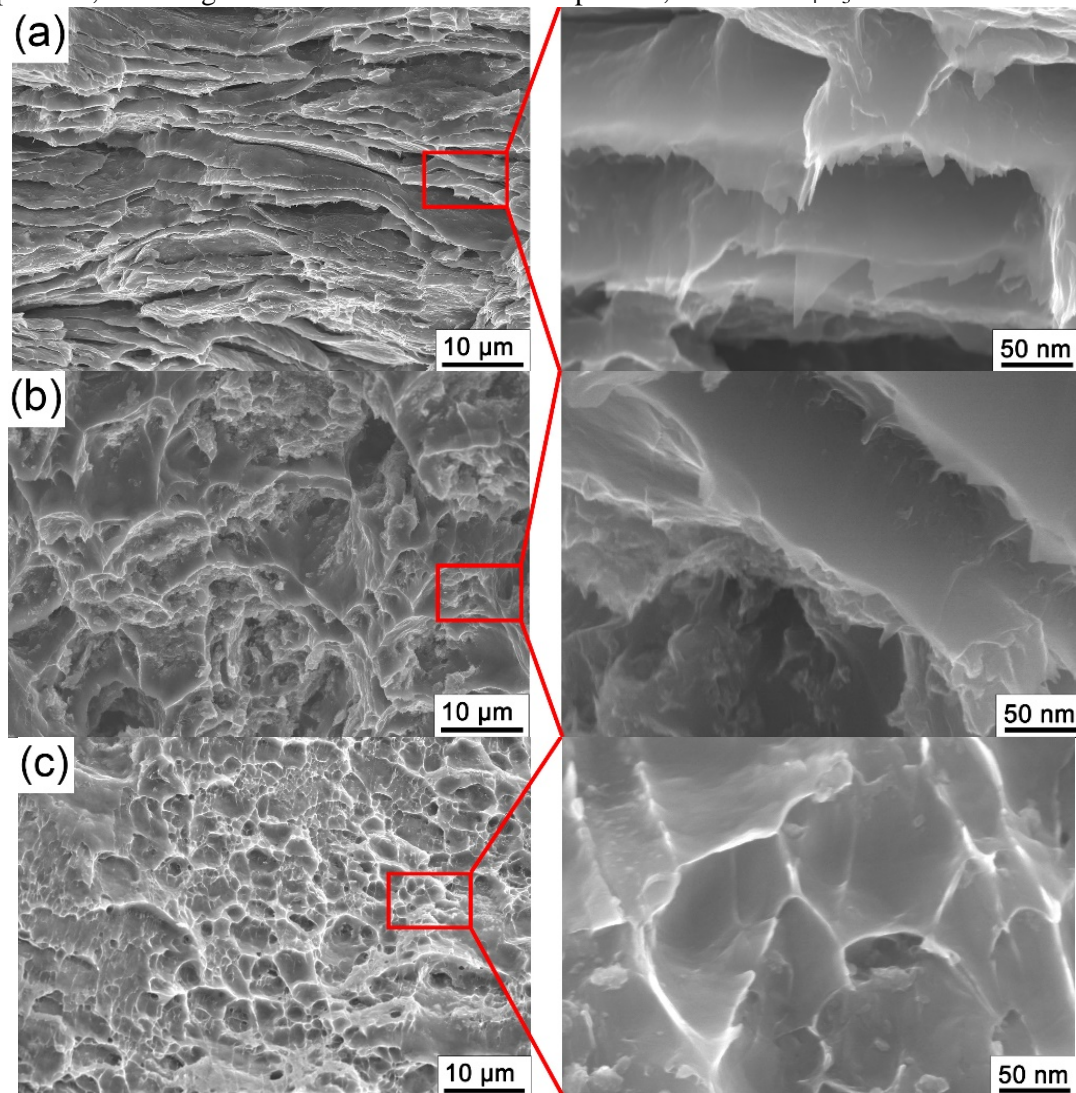


**Fig. 2** Tensile fractograph of (a) Composite I, (b) Composite II, and (c) pure Al I

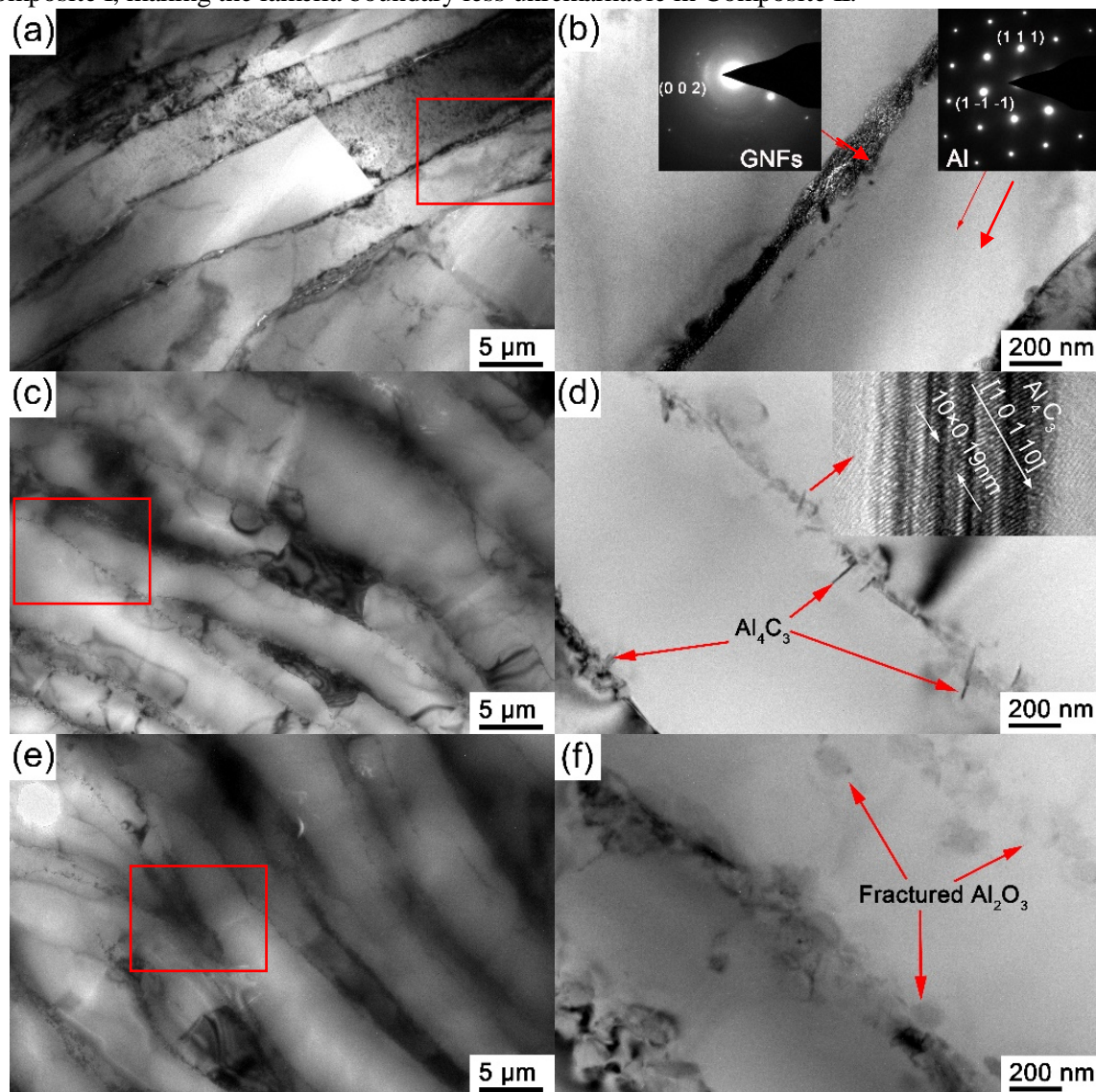
### 3.3. Microstructures

Fig. 3 exhibits the low- and high-magnification TEM images of Composite I, Composite II, and Pure Al I viewed on the longitudinal section. The low-magnification TEM images show that all three materials possess lamellar structure in the whole, due to the rearrangement of aluminum flakes under the axial pressure applied during the SPS process. It is worth noticing that the thicknesses of



aluminum layers in all three samples are almost the same. In addition, the lamella boundary in Composite I is more distinct than those in Composite II and Pure Al I.

The high-magnification TEM images with their selected area electron diffraction (SAED) or high-resolution (HR)-TEM inserted in Fig. 3 exhibit obviously different structures sandwiched between these aluminum lamellas: continuous GNFs dispersed in Composite I (Fig. 3(b)), discontinuous GNFs and an amount of needle-shaped  $\text{Al}_4\text{C}_3$  immersed in Composite II (Fig. 3(d)), and fractured amorphous  $\text{Al}_2\text{O}_3$  on Pure Al I (Fig. 3(f)). Masses of needle-shaped  $\text{Al}_4\text{C}_3$  in Composite II consume a large number of GNFs, thus there is less GNFs between the aluminum lamellas in Composite II than in Composite I, making the lamella boundary less unremarkable in Composite II.



**Fig. 3** TEM of (a) Composite I and (b) magnified map of rectangular zone in (a) (SAED of GNFs and Al matrix are inserted); (c) Composite II and (d) magnified map of rectangular zone in (c) ( $\text{Al}_4\text{C}_3$  are marked by arrows and HRTEM of  $\text{Al}_4\text{C}_3$  are inserted); (e) Pure Al I and (f) magnified map of rectangular zone in (e) ( $\text{Al}_2\text{O}_3$  are marked by arrows).

Study on carbon fiber reinforced aluminum composite find that the carbon-aluminum interface reaction generally occurs at temperatures higher than 500 °C [16]. In the current work, the sintering

parameters except the sintering time are the same for all materials, and the sintering temperature is higher than 500 °C. Then, the interface reaction is determined by the sintering time. With a shorter sintering time (4 min), the interface reaction is suppressed, while it is fully carried out with an extended sintering time of 8 min. Thus, the existence of sufficient  $\text{Al}_4\text{C}_3$  phase is the basic distinction between Composite I and II, which further leads to their different mechanical properties. The mechanical test results show that the strength of Composite I is obviously improved compared to its Al matrix, while that of Composite II changes very little and its elongation declines. Hence, the mass interface reaction phase of  $\text{Al}_4\text{C}_3$  spoiled the mechanical properties of the GNFs/Al composites. To obtain graphene-enhanced aluminum composites, the mass interface reaction should be avoided during the fabrication process.

To understand the strengthening mechanism of GNFs/Al composites, the interface characteristics of Composite I were further studied by HRTEM. The observation demonstrated that two types of GNFs/Al interfaces exist in the composite, as displayed in Fig. 4(a) and (b). The image in Fig. 4(a) shows that the GNFs and the aluminum matrix are separated by an  $\text{Al}_2\text{O}_3$  layer. The  $\text{Al}_2\text{O}_3$  layer covers the aluminum particles due to the oxidation of aluminum in air, and it is difficult to remove even during ball milling [17, 18]. The pulse may partially fracture the  $\text{Al}_2\text{O}_3$  layers during the SPS process [19, 20]. In these fractured areas, direct contact between GNFs and the matrix is feasible, as shown in Fig. 4(b). From Fig. 4(a) and (b), we can see that the interfaces between GNFs and aluminum matrix are tightly bonded on the atomic scale, whether there is an  $\text{Al}_2\text{O}_3$  layer between them or not. This well-dispersed and compactly bonded interface between GNFs and aluminum matrix facilitates the stress transfer and effectively hinders dislocation movement, which are very important for the strengthening effect of GNFs to be fully realized.

The characteristic of the GNFs in Composite I was also studied by Raman spectroscopy, and compared to the original GNFs powder at the same condition. In the averaged Raman spectra in Fig. 4(c), the D peak at  $1350\text{ cm}^{-1}$  indicates the disorder of carbon material, and its intensity ratio to the G peak at  $1580\text{ cm}^{-1}$  ( $I_D/I_G$ ) is a measure of defects in graphene. The obvious D and G bands in the bottom line confirm the existence of GNFs in Composite I, and the lower value of  $I_D/I_G$  in the bottom line indicates that the fabrication process did not destroy the structure of GNFs in the aluminum matrix.

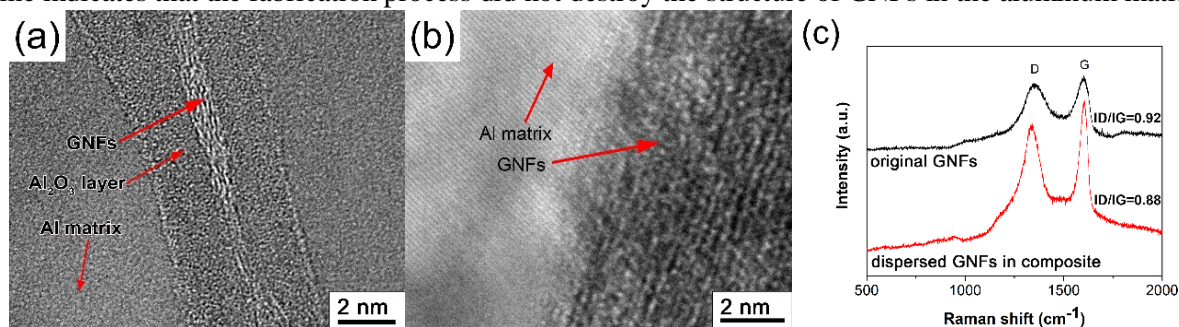


**Fig. 4** (a) (b) HRTEM of two kind GNFs/Al interface in Composite I ;  
(c) Raman spectra of the original GNFs and dispersed GNFs in Composite I .

Based on the above-mentioned fracture surface morphology and microstructure analyses, the structural features of Composite I with enhanced mechanical properties can be described as follows: regular lamellar structure composed of the alternating arrangement of GNFs and aluminum flakes, compact GNFs/Al interface bonded at the atomic scale, and that reinforced phase almost maintains the original structure.

Through the microstructure study, the higher strength in composite I can be attributed to two reasons. First, the reinforcement bears partial stress transferred from the matrix. The dispersed and compactly bonded interface between GNFs and aluminum matrix promotes the stress transfer from the matrix to GNFs. When the GNFs are oriented parallel to the tensile direction, the stress load is aligned with the strongest direction of the GNFs. Therefore, GNFs in the composite with well-maintained raw

structure can effectively bear the partial stress transferred from the aluminum matrix. Second, dislocation pile-up, which takes place during the plastic deformation, could be hindered by the reinforcement. The uniform distribution of the GNFs and the compact bonded interface in the composite effectively hinder the dislocation movement. In a word, the GNFs/Al Composite I has remarkably enhanced mechanical properties, because its elaborated structure can bear the partial stress transferred from the matrix and effectively hinder the dislocation movement.

The shorter strain with the steady flow and negligible necking region in Composite I during the tensile process may be attributed to microcracks, which may nucleate for two reasons. Some microcracks are formed within the material due to impurities or voids introduced during the manufacturing process, and others can be caused by stress concentration. As Composite I is dense and uniform, the microcracks mainly stem from stress concentration with severe dislocation pile-up at the GNFs/Al interface, which results in short plastic strain and negligible necking. On the other hand, the good structure of Composite I allows the composite to retain relative high plasticity with a total strain of 14.5%.

#### 4. Conclusions

In the present research, GNFs/Al composites with 1.0 wt.% GNFs, which possess high relative density (near 100%) and homogenous structure, were successfully fabricated by a ball milling and SPS method. The microstructure, interface characteristics, and fracture morphology of two composites with different tensile mechanical properties were systematically investigated. The major conclusions are as follows:

- (1) The mechanical properties of GNFs/Al composites depend dramatically on the characteristics of the GNFs-aluminum interface. Mass interfacial reaction reduces the mechanical properties of the composites.
- (2) The good mechanical properties of the enhanced GNFs/Al composites can be ascribed to the fact that the structure of the raw reinforcement is well-maintained: the GNFs are distributed uniformly and parallel to the tensile direction, the absence of mass interfacial reaction, and the good interface bonding in the composite. These factors, taken together, allow the high strength and the fine flexibility of the GNFs to be fully utilized to enhance the composites.
- (3) SPS parameters have important effects on the interfacial characteristic and mechanical properties of GNFs/Al composites. A long sintering time should be avoided, as it is likely to induce undesirable interface reactions.

#### Acknowledgments

The authors thank the financial support from Technology Innovation Fund of China Aviation Industry Corporation.

#### References

- [1] Geim A K 2010 *Graphene: Status and Prospects. International of Vacuum Congress* p1530.
- [2] Lee C, Wei X, Kysar J W and Hone J 2008 *Science* 321 385
- [3] Tsai J L and Tu J F 2010 *Mater. Des.* 31 194
- [4] Zheng Q, Geng Y, Wang S, Li Z and Kim J K 2010 *Carbon* 48 4315
- [5] Li B and Zhong W H 2011 *J. Mater. Sci.* 46 5595
- [6] Walker L S, Marotto V R, Rafiee M A, Koratkar N and Corral E L 2011 *Acs Nano* 5 3182
- [7] Chen Q, Zhang L and Chen G 2012 *Anal. Chem.* 84 171
- [8] Bartolucci S F, Paras J, Rafiee M A, Rafiee J, Lee S and Kapoor D 2011 *Mater. Sci. Eng. A* 528 7933
- [9] Yan S J, Dai S L, Zhang X Y, Yang C, Hong Q H, and Chen J Z 2014 *Mater. Sci. Eng. A* 612 440
- [10] Li Z, Guo Q, Li Z, Fan G, Xing D B, and Su Y 2015 *Nano Let.* 15 8077
- [11] Shin S E, Choi H J, Shin J H, and Bae D H 2015 *Carbon* 82 143
- [12] Liu G, Zhao N, Shi C, Liu E, He F and Ma L 2017 *Mater. Sci. Eng. A* 699 185

- [13] Feng S, Guo Q, Li Z, Fan, G, Li, Z and Xiong D B 2017 *Acta Mater.* 125 98
- [14] Hajjari E, Divandari M and Mirhabibi AR 2010 *Mater. Des.* 31 2381
- [15] Wang X, Chen GQ, Li B, Wu GH and Jiang DM 2009 *J. Mater. Sci.* 44 4303
- [16] Lalet G, Kurita H, Miyazaki T, Kawasaki A and Silvain J F 2014 *Mater. Let.* 130 32
- [17] Liao J Z, Tan M J and Sridhar I. *Mater. Des.* 31 S96
- [18] Lee M, Choi Y, Sugio K, Matsugi K and Sasaki G. 2014 *Compos. Sci. Tech.* 97 1
- [19] Lalet G, Kurita H, Miyazaki T, Kawasaki A and Silvain J F. 2014 *Mater. Let.* 130 32
- [20] Xie G, Ohashi O, Chiba K, Yamaguchi N, Song M, Furuya K and Noda T 2003 *Mater. Sci. Eng. A* 359 384